

**CHAPTER V**  
**DILUTE SOLUTION PROPERTIES OF HEXANOYL CHITOSAN**  
**IN CHLOROFORM, DICHLOROMETHANE,**  
**AND TETRAHYDROFURAN**

**5.1 ABSTRACT**

Hexanoyl chitosans (H-chitosan) were synthesized using a new method to obtain the organic solvent soluble chitosan derivatives. H-chitosan with degree of substitution (DS) of 3.92 was dissolved in selective organic solvents such as chloroform, dichloromethane and tetrahydrofuran in order to study the effect of solvent type on hexanoyl chitosan solution properties. The solution properties of hexanoyl chitosan were determined by dilute solution viscometry, dynamic light scattering, and surface tension technique. The calculated solubility parameter of H-chitosan was estimated to be 9.31 in  $(\text{cal}\cdot\text{cm}^{-3})^{0.5}$ , a value closer to the solubility parameter value of chloroform than those of dichloromethane and tetrahydrofuran. Intrinsic viscosity values of H-chitosan dissolved in chloroform, dichloromethane or tetrahydrofuran were determined by the Huggins-Kramer extrapolation and found to be  $\sim 1.377$ ,  $1.478$ , and  $1.385$  dl/g, respectively. The  $k_H$  values for H-chitosan in each solution indicate that the three H-chitosan solutions possess similar polymer-solvent interactions. The hydrodynamic radius,  $R_H$  value, in chloroform appears to be larger than those in dichloromethane and tetrahydrofuran, suggesting that more free unwinding of the polymer chain occurs in chloroform. Surface tension values of H-chitosan dissolved in chloroform and tetrahydrofuran decrease with increasing concentration. On the contrary, surface tension of H-chitosan dissolved in dichloromethane increases with increasing concentration.

**(Key-words:** hexanoyl chitosan; solution properties; viscosity; dynamic light scattering; surface tension; solvent)

## 5.2 INTRODUCTION

Ability to dissolve chitosan in organic solvents is important in many applications. It is well known that chitosan is generally insoluble in many common solvents: water, alkali and organic solvents, but it is soluble in solutions of organic acids only when the pH of the solution is less than 6 [1]. Acetic and formic acids are two of the most widely used solvents for dissolving chitosan. However, these solvents offer only very limited applications in producing chemical derivatives in homogeneous solution, in particular the large-scale applications. Poor solubility of chitosan in common organic solvents can be traced to its rigid crystalline structure through intramolecular and intermolecular hydrogen bondings [2]. This is the primary reason for limited useful chitosan applications. In order to solve this problem, chemical modification of chitosan is thus required.

Solubility of chitosan derivatives in organic solvents is essential in designing novel molecular structures as functional materials. There has been several works that have been carried out on chemical modifications on the chitosan structure [3-7]. Chemical modifications to introduce hydrophobic nature into chitosan such as phthaloylation [3], alkylation [4], and acylation [5-7] reactions can be carried out. Organic soluble derivatives of chitosan can be used to formulate by-designed materials for biomedical applications such as polymeric drugs and artificial organs with high specificity and wide applicability. Acylated chitosans are soluble in various organic solvents, such as chloroform, benzene, pyridine, and tetrahydrofuran. *N*-acylated chitosan has been fabricated as membranes [8], fibers [9], and films [10]. *N*-hexanoyl chitosan was found to exhibit the best blood compatibility in comparison with *N*-propionyl, *N*-butyryl, and *N*-pentanoyl chitosans [11]. Furthermore, *N*-hexanoyl and *N*-octanoyl chitosans were found to be anti-thrombogenic and resistant to the hydrolysis by lysozyme [12]. Thus, acylated chitosan is an interesting chitosan derivative suitable for biomedical applications.

Previous report has dealt with characterizations of acylated chitosans, i.e. hexanoyl chitosan (H-chitosan), decanoyl chitosan (D-chitosan) and lauroyl chitosan (L-chitosan) in solid state [7]. The acyl side chains in H-, D-, and L-chitosans should assemble into a similar layered structure. The layer spacing,  $d$  increased linearly

with increasing length of the acyl substituents. In spite of these studies, the dilute solution properties and surface tension of the acylated chitosan, H-chitosans, have not been investigated.

The present work focuses on the dilute solution behavior of H-chitosan in organic good solvents, i.e. chloroform, dichloromethane, or tetrahydrofuran through viscometry and dynamic light scattering technique. Our results demonstrate the importance of solvent and polymer-solvent interactions and provide an explanation for some poorly understood experimental observations in organic soluble chitosan derivatives studies. The study on the surface tension of H-chitosan in selected solvents will also be reported.

### 5.3 EXPERIMENTAL

#### Materials

Shrimp shell was kindly supplied by Surapol Food Co., Ltd. Sodium hydroxide solution 50% (w/w) was kindly supplied by KPT Cooperation, Thailand. The molecular weights of chitin and chitosan were determined by the viscometric method. The viscosity-average molecular weight of chitin and chitosan were found to be  $8.21 \times 10^5$  and  $3.72 \times 10^5$ , respectively.

Hexanoyl chloride was purchased from Fluka Co., Ltd. Pyridine, chloroform and methanol were purchased from Labscan Co., Ltd. Pyridine and chloroform were distilled and dried over molecular sieve prior to use. Other chemicals were of analytical grade and were used without further purification. The organic solvents used in this study were chloroform, dichloromethane and tetrahydrofuran (Labscan Co., Ltd). Table 5.1 lists the properties of the selected organic solvents.

#### H-chitosan Preparation

Chitosan was soaked in pyridine for a period of one week, and filtered off before further soaking in a mixture of pyridine and chloroform for a period of one day. The mixture was cooled to  $-10^\circ\text{C}$  in an ice-salt bath, and then hexanoyl chloride dissolved in chloroform was added dropwise in during a period of 2 h. The mixture was then stirred for 2 h at room temperature and further refluxed for 6 h at  $98^\circ\text{C}$ . A

heterogeneous aggregation of the product was observed in the mixture. The resultant mixture was poured into methanol, and the precipitated product was filtered off. The product was dissolved again in chloroform, then precipitated by pouring into methanol, filtered off, extracted in a Soxhlet extractor with methanol for 8 h, and dried in vacuum oven at 40°C for 24 h. The sticky yellowish product was obtained.

The drying acylated derivatives of chitosan, fresh pyridine, and chloroform were placed in a flask in the amount described above. This procedure was repeated several times in order to vary the degree of substitution of the resultant hexanoyl chitosan (Figure 5.1) [7].

### Characterization

FTIR spectroscopic analysis was conducted using a Bruker spectrometer (EQUINOX55) with a resolution of 4 cm<sup>-1</sup>. <sup>1</sup>H-NMR spectrum was recorded by using FT-NMR 500 MHz spectrometer (JEOL, JNM-A500). H-chitosan was dissolved in CDCl<sub>3</sub> and tetramethylsilane (TMS) was used as the reference for the chemical shift measurement. Elemental analysis data were obtained from a CHNS/O analyzer (Perkin Elmer PE2400 Series II: option CHN) with the combustion temperature set at 950°C. The sample (1-2 mg) was filled in a tin foil sheet and analyzed under air with oxygen as the combustion gas (flow rate of 20 ml/min) and He as the carrier gas (flow rate of 200 ml/min).

### Solution Properties

#### Method of Estimation of Solubility Parameter by Group Contribution

The method for determining solubility parameters involves a calculation based on so called the group contribution [13]. The essence of this approach is to assume that a molecule can be “broken down” into a set of functional groups. To calculate the solubility parameter of a polymer one uses the simple relationship:

$$\delta = \frac{\sum_i F_i^*}{\sum_i V_i^*} (\text{cal.cm}^{-3})^{0.5} \quad (1)$$

where  $F_i^*$  is the molar attraction constant of the  $i^{\text{th}}$  group, while  $V_i^*$  is the corresponding molar volume constant of this group [13].

### Intrinsic Viscosity Measurement

Intrinsic viscosity  $[\eta]$  is a measurement of the inherent ability of a polymer to increase solution viscosity. In the dilute regime, solution viscosity can be represented by a power series of polymer concentration  $c_p$ :

$$\eta = \eta_s(1 + [\eta]c_p + k_H[\eta]^2c_p^2 + \dots) \quad (2)$$

where  $\eta_s$  is the solvent viscosity and  $k_H$  is the Huggins coefficient. The intrinsic viscosity can be determined by measuring viscosity of solutions at low concentrations and extrapolating the viscosity in the limit of infinite dilution, according to the Huggins or Kraemer relationship, respectively [14].

$$\eta_{sp}/c_p = [\eta] + k_H[\eta]^2c_p \quad (3)$$

$$\ln(\eta_r)/c_p = [\eta] + k_K[\eta]^2c_p \quad (4)$$

where  $\eta_{rel}$  is the relative viscosity, defined as the ratio of solution viscosity and solvent viscosity  $\eta/\eta_s$ , and  $\eta_{sp}$  is the specific viscosity which can be defined as  $(\eta_r - 1)$ .

H-chitosan solutions of various concentrations (0.1-0.5 g/dl) in different organic solvent were prepared. Each solution was passed through a filter (PTFE, 0.2  $\mu\text{m}$ ) to remove insoluble materials. The capillary viscometer (Cannon-Fenske, No 50) was filled with 5 ml of solution and thermally equilibrated in a water bath to maintain a fixed temperature at  $30 \pm 0.1^\circ\text{C}$ . The sample was passed through the capillary once before the running time was measured. For each sample, viscosity was measured 3 times.

### Light Scattering Measurement

Dynamic light scattering measurement was carried out at the temperature of  $30^\circ\text{C}$ , using a Malvern dynamic light scattering spectrometer with a PCS7 stepper motor controller, a PCS8 temperature controller, and a photo multiplier.

In dynamic light scattering experiments a normalized time autocorrelation function  $g_2(\tau, q)$  of the scattered intensity was measured [15]:

$$g_2(\tau, q) = \frac{\langle I^*(0, q)I(\tau, q) \rangle}{\langle I(0, q)^2 \rangle} \quad (5)$$

where  $I(\tau, 0)$  is the scattering intensity at a certain delay time from a reference time  $t = 0$ . In dilute solutions  $g_2(\tau, 0)$  can be expressed in terms of the normalized field correlation function  $g_1(\tau, q)$  using the Siegert relationship

$$g_2(\tau, q) = 1 + \beta |g_1(\tau, q)|^2 \quad (6)$$

where the coefficient  $\beta < 1$  is the coherence factor. For short delay times  $g_1(\tau, q)$  is well approximated by a single-exponential decay:

$$g_1(\tau, q) \approx \exp(-\Gamma(q)\tau) \text{ if } \Gamma(q)\tau < 1 \quad (7)$$

This decay rate  $\Gamma(q)$  is related to an apparent mutual diffusion coefficient as [15, 16]

$$\Gamma(q) = q^2 D_{app}(c, q) \quad (8)$$

where

$$D_{app}(c, q) = D_{cm}(1 + CR_g^2 q^2 - \dots) \quad (9)$$

$D_{cm}$  is the diffusion coefficient of the particle's center of mass, where the subscript indicates the z-average over the molar mass distribution and  $q$  is the wavevector defined by  $q = (4\pi/\lambda)n_o \sin(\theta/2)$  with  $n_o$  the refractive index,  $\theta$  the scattering angle, and  $\lambda$  the wavelength of incident light.  $D_{cm}$  depends on concentration and is well represented by a linear relation:

$$D_{cm} = D_{cm}(1 + k_D c_p) \quad (10)$$

where  $k_D$  is the first-order concentration coefficient which depends on the second virial coefficient,  $A_2$ , and the hydrodynamic friction coefficient,  $\zeta_l$ , given by [14]

$$k_D = 2A_2 M - \zeta_l - \nu_{sp} \quad (11)$$

where  $M$  is molecular weight of polymer., and  $\nu_{sp}$  is the reciprocal of density of polymer.

The ratio  $\Gamma(q)/q^2 = D_{app}(c, q)$  is angular dependent and thus an apparent diffusion coefficient which is valid for small  $q^2 R_g^2 < 2$ . This angular dependence results from segmental motions and polydispersity.

The double extrapolation of  $D_{app}(c, q)$  in the limits of  $c=0$  and  $q=0$  can be alternatively done in a dynamic Zimm plot, giving the diffusion coefficient at infinite dilution,  $D_o$ , from which the hydrodynamic radius,  $R_H$ , can be obtained from the Stokes-Einstein relationship

$$R_H = \frac{K_B T}{6\pi\eta D_o} \quad (12)$$

where  $\eta$  is the solvent viscosity and  $k_B T$  is the Boltzmann constant multiplied by the absolute temperature.

#### Surface Tension Measurement

Surface tension of polymer solution was measured by using a Kruss Drop Shape analyzer (Kruss Co., Germany) at 30°C.

### 5.4 RESULTS AND DISCUSSION

#### **Characterization of H-Chitosan**

H-chitosan was synthesized and its chemical structure was characterized by FT-IR,  $^1\text{H-NMR}$  and elemental analysis.

The FT-IR spectra of chitosan and H-chitosans, prepared by repeatedly allowing the hexanoylation reaction up to four times, are shown in Figure 5.2. The characteristic absorption at 3000~4000  $\text{cm}^{-1}$  (OH,  $\text{NH}_2$ ) in the FT-IR spectrum of the chitosan were absent in the spectrum of H-chitosan of the four times reaction. The spectra of the hexanoyl chitosan also show new characteristic absorptions at 1717  $\text{cm}^{-1}$  (C=O of  $\text{N}(\text{COR})_2$ ), 1749  $\text{cm}^{-1}$  (C=O of OCOR), 2958  $\text{cm}^{-1}$ , 2932  $\text{cm}^{-1}$  ( $\nu_{\text{as}}$   $\text{CH}_2$ ), 2873  $\text{cm}^{-1}$  ( $\nu_{\text{s}}$   $\text{CH}_2$ ), 1458  $\text{cm}^{-1}$  ( $\delta$   $\text{CH}_2$ ), and 1171  $\text{cm}^{-1}$  (twisting vibration of  $\text{CH}_2$ ). These characteristic absorption peaks of the hexanoyl chitosan became sharper as the number of the repeated reaction was increased. The characteristic absorption peaks of the chitosan which generally can be observed at 3000~4000  $\text{cm}^{-1}$  (OH,  $\text{NH}_2$ ) are absent in the FT-IR spectra of the H-chitosan, indicating that the hexanoylation reaction occurred at the hydroxyl groups of the chitosan. The FT-IR data suggest that the hexanoyl groups were substituted into the hydroxyl and amino groups on the monosaccharide units of the chitosan.

$^1\text{H-NMR}$  data was taken to confirm the chemical structure of H-chitosan.  $^1\text{H-NMR}$  spectra of the H-chitosan in  $\text{CDCl}_3$  (Figure 5.3) show signals at 5.6 (H1), 5.2 (H3), 4.2 (H4), 3.4~3.6 (H6, H5), and 2.6 (H2) ppm due to the protons of the polysaccharide ring and the signals at 2.4 (-CO- $\text{CH}_2$ ), 1.3-1.6 (- $\text{CH}_2$ -) and 0.9 (- $\text{CH}_3$ ) ppm are assigned to the peaks of hexanoyl chains.

From FT-IR and  $^1\text{H-NMR}$  analysis, the data clearly suggest that H-chitosan was obtained after the chemical modification of chitosan by the hexanoylation reaction.

The degree of substitution of H-chitosan was 3.92 for the four times reaction, based on the data obtained from the elemental analysis. Experimental results were compared with the calculated values, and the degree of substitution was determined based on the C/N ratio of the product.

### **Solubility Parameter of H-Chitosan**

The solubility parameter ( $\delta$ ) is an important property of polymer which is defined as the square root of cohesive energy density. Solubility parameters provide an easy numerical method of rapidly predicting the extent of interaction between materials, particularly liquids and polymers. They are useful in ensuring the suitability of polymers for practical applications and in formulating blends of solvents for particular purposes. The group contribution method for calculate the solubility parameter of polymers is based on the contributions from individual groups, atom and bonds constituting the molecules. Based on the structure of the H-chitosan, one can estimate the solubility parameter value by the group contribution method [13]. H-chitosan consists of  $-\text{N}<$ ,  $-\text{CH}$ ,  $-\text{CH}_2$ ,  $-\text{CH}_3$ ,  $-\text{O}-\text{C}=\text{O}$ ,  $-\text{C}=\text{O}$ ,  $-\text{O}-$ . This is schematically shown in Figure 5.1. Table 5.2 gives the molar volume constants and the molar attraction constants of various groups of the H-chitosan. The calculated solubility parameter of H-chitosan was estimated to be 9.31 in  $(\text{cal}\cdot\text{cm}^{-3})^{0.5}$ . This estimated value can be compared with those published values of chloroform, dichloromethane and tetrahydrofuran which were used as the solvents. The solubility parameter value of the H-chitosan is closest to the solubility parameter value of chloroform more than those of dichloromethane and tetrahydrofuran.

### **Dilute Solution Properties of H-Chitosan**

#### Intrinsic Viscosity

The properties of dilute solutions are governed by the properties of individual macromolecules, unlike in concentrated solutions where the chains are entangled with each other. For the dilute solution, the Huggins equation is the most appropriate



one to determine the intrinsic viscosity and the Huggins constant, which could then be used to study the hydrodynamic volume of polymers chains and the interaction between difference polymer chains or between polymer chains and the solvent [17].

Table 5.3 lists the intrinsic viscosity and Huggins coefficient of H-chitosan solutions. Intrinsic viscosity values of the H-chitosan dissolved in chloroform, dichloromethane and tetrahydrofuran were determined by the Huggins-Kramer extrapolation of the regression lines and found to be  $\sim 1.377 \pm 0.008$ ,  $1.478 \pm 0.003$ , and  $1.385 \pm 0.003$  dl/g (Figure 5.4), respectively. These data suggest that the polymer-solvent interaction of the H-chitosan with each solvent is comparable in magnitude.

The Huggins coefficient,  $k_H$  is a measure of polymer-polymer interactions in solution. Experimentally, the Huggins coefficient is independent of molecular weight for long chains, with values of roughly 0.30-0.40 for good solvents and 0.50-0.80 for  $\theta$  solvents. The higher  $k_H$  value means that the interactions between difference molecules become stronger.  $k_H$  assumes high values when intermolecular association exists [18]. The  $k_H$  values for the H-chitosan in chloroform, dichloromethane and tetrahydrofuran solutions are 0.427, 0.473, and 0.508, respectively, suggesting that the three H-chitosan solutions contain similar polymer-solvent interactions. The  $k_H$  values for these systems show that they are good solvents.

Finally, we show the Utracki-Simha plot [19],  $\eta_{sp}$  versus  $c \cdot [\eta]$ , in Figure 5.5. In dilute regime, the polymer chains are separated from each other and the interactions are weak, so that the plot and the collapse of the data validate the correctness of the Huggin's equation.

### Dynamic Light Scattering

The dynamic light scattering experiment was carried out on solutions of the H-chitosan in the three solvents (chloroform, dichloromethane and tetrahydrofuran). Measurements were taken at the wavelength of 514.5 nm and at 30°C. The results are shown in Figure 5.6. Values of  $D_0$ ,  $k_D$ , the normalized second cumulant,  $\mu_2/\Gamma^2$  as well as the hydrodynamic radius,  $R_H$  from the stokes-Einstein relationship are listed

in Table 5.4.  $R_H$  values are 50.1, 38.5, and 39.9 nm for chloroform, dichloromethane and tetrahydrofuran, respectively. This suggests that the H-chitosan chain expands the most in chloroform.

$k_D$  is the constant describing the concentration dependence of the diffusion coefficient. It is well known that [14] in a sufficiently good solvent the diffusion coefficient increases with polymer concentration. As the solvent quality becomes poorer,  $k_D$  becomes eventually negative. From Table 5.4, for all samples,  $k_D$  values are in the positive range, indicating that all the solvent investigated are good solvents for the H-chitosan.  $k_D$  values also support the result of  $k_H$  as determined by viscometry

The normalized second cumulant,  $\mu_2/\Gamma^2$ , indicating size polydispersity, is shown in Table 5.4 [20]. For chloroform solution, the normalized variance,  $\mu_2/\Gamma^2$ , is 0.61, higher than those of the other solutions, indicating that the degree size difference of H-chitosan molecules in chloroform is higher than those in dichloromethane or tetrahydrofuran solution [20]. The normalized second cumulant values for dichloromethane and tetrahydrofuran are 0.40 and 0.38, respectively, indicating the degrees of size mismatch for these solvents are comparable.

The  $R_H$  values recorded in chloroform appear larger than those in dichloromethane and tetrahydrofuran, suggesting that some unwinding of the polymer chain occurs in chloroform. This can be related to the solubility parameter of H-chitosan and chloroform. Our results are in good agreement with the earlier experiment of dynamic light scattering of poly(*p*-methoxy)phenyl acetylene in chloroform [21,22].

The light scattering data indicate that the variation of hydrodynamic radius of H-chitosan in different organic solvent could be due to the different polymer conformation in solution. A polymer/solvent interaction is operating here leading to different  $R_H$  values. It must be noted, as pointed out by Lee and coworker [23], that the hydrodynamic radius is not strictly the same as the chain dimension, but depending on the chain flexibility. This implies that the chain flexibility may vary with solvent, resulting in a more compact structure with a lower hydrodynamic radius.

Finally, Figure 5.7 shows that  $D_0$  is inversely proportional to the solvent viscosity. This implies a stokes-Einstein relationship.

### Surface Tension

Another interesting feature, which has rarely been investigated, concerns the surface and interfacial activities of the hydrophobically modified chitosan, H-chitosan. The surface tension of H-chitosan solutions in different organic solvents could be measured by the pendant drop method. Geometry of a drop was analyzed optically (Figure 5.8). The surface tension of a system is governed by the usual thermodynamic variables and primarily by the chemical nature of the components present in the surface phase. The surface activity phenomenon can be used to explain its molecular picture (i.e., the nature of its monomeric units, its orientation, and overall distribution in solvent medium as well as interaction with the solvent molecule).

Figure 5.9 shows surface tension vs. concentration for the three organic solvents of H-chitosan. Surface tensions of H-chitosan dissolved in chloroform and tetrahydrofuran generally decrease with increasing concentration, and no maxima or minima can be observed. The decrease in surface tension could be attributed to the increase adsorption of the variable H-chitosan molecules at the air-solution interface as the polymer concentration increases leading to the interfacial excess of the polymer. At low H-chitosan concentrations, H-chitosan molecules adsorb at the interface so that the H-chitosan molecules can escape into the air phase because of insufficient number of the H-chitosan molecules are available to form intermolecular aggregates. As a result, a sharp decrease in surface tension is observed in the lower polymer concentration range. In the higher H-chitosan concentration range, the interface becomes saturated with H-chitosan molecules and the intermolecular aggregates start to provide a favorable environment for the hydrophobes. Consequently, a less pronounced decrease in surface tension can be observed in the higher H-chitosan concentration range. On the other hand, the surface tension of H-chitosan dissolved in dichloromethane increases with increasing concentration.

## 5.5 CONCLUSIONS

Hexanoyl chitosan with DS of 3.92 was dissolved in various organic solvents such as chloroform, dichloromethane and tetrahydrofuran in order to study the effect of solvent on solution properties of the hexanoyl chitosan. Dilute solution properties of H-chitosan in three organic solvents, chloroform, dichloromethane or tetrahydrofuran were studied to investigate the relationship between polymer-solvent interaction, the solution viscosity and hydrodynamic radius, and the air-liquid interfacial activities. The  $k_H$  values for the H-chitosan in each solution indicates that the three H-chitosan solutions contain comparable polymer-solvent interactions as they are expected to be for a good solvent. The  $R_H$  value determined in chloroform appears to be larger than those in dichloromethane and tetrahydrofuran, suggesting that a more favorable unwinding of the polymer chain occurs in chloroform. This can be related to the closeness between the solubility parameters of H-chitosan and chloroform. Surface tension of H-chitosan dissolved in chloroform and tetrahydrofuran decreases with increasing concentration, whereas the surface tension of the H-chitosan dissolved in dichloromethane increases with increasing concentration.

## 5.6 ACKNOWLEDGMENTS

The authors would like to acknowledge the grant provides by Chulalongkorn University through the Ratchadaphiseksomphot Endowment Fund, and the Conductive and Electroactive Research Unit of Chulalongkorn University. The authors wish to thank partial support from the Petroleum and Petrochemical Technology Consortium (through a governmental load from the Asian Development Bank) and from the Petroleum and Petrochemical College, Chulalongkorn University.

## 5.7 REFERENCES

- [1] Muzzaerelli, R. A. A. *Chitin*, Pergamon Press, Oxford, UK, 1977.
- [2] Roberts, G. A. F. *Chitin Chemistry*; Palgrave Macmillan: London, 1992.
- [3] Nishimura, S. I.; Kohgo, O.; Kurita, K. *Macromolecules* 1991, 24, 4745.
- [4] Yaipani, M.; Hall, L. D. *Macromolecules* 1984, 17, 272.
- [5] Hirano, S.; Ohe, Y.; Ono, H. *Carbohydrate Research* 1976, 47, 315.
- [6] Moore, G. K.; Roberts, G. A. F. *International Journal of Biological Macromolecules* 1981, 3, 292.
- [7] Zong, Z.; Kimura, Y.; Takahashi, M.; Yamane, H. *Polymer* 2000, 41, 899.
- [8] Seo, Y.; Ohtake, H.; Unishi, T.; Iijima, T. *Journal of Applied Polymer Science* 1995, 58, 633.
- [9] Hirano, S.; Usutani, A.; Yoshikawa, M.; Midorikawa, T. *Carbohydrate Polymers* 1998, 37, 311.
- [10] Xu, D.; McCarthy, S. P.; Gross, R. A.; Kaplan, D. L. *Macromolecules* 1996, 29, 3436.
- [11] Lee, K. Y.; Ha, W. S.; Park, W. H. *Biomaterials* 1995, 16, 1211.
- [12] Hirano, S.; Noishiki, Y. *Journal of Biomedical Materials Research* 1985, 19, 413.
- [13] Painter, P. C.; Colerman, M. M. *Fundamentals of Polymer Science: An Introductory Text*, Technomic Publishing Co., Inc.: Pennsylvania, 1997.
- [14] Teraoka, I. *Polymer Solutions: An Introduction to Physical Properties*, John Wiley and Sons, Inc., New York, 2002.
- [15] Berne, B. J.; Pecora, R. *Dynamic Light Scattering*, Wiley & Sons: New York, 1976.
- [16] Zimm, B. H. *Journal of Chemistry and Physics*, 1948, 16, 1099.
- [17] Zhang, Y. X.; Da, A. H.; Butler, G. B.; Hogen-Esch, T. E. *Journal of Polymer Science: Part A: Polymer Chemistry*, 1992, 30, 1383.
- [18] Bohdanecky, M.; Kovar, J. *Viscosity of Polymer Solutions*; Elsevier Scientific Publishing Company: Amsterdam, 1982.
- [19] Utraki, L.; Simha, R. *Journal of Polymer Science: Part A*, 1963, 1, 1089.
- [20] Patterson, P. M.; Jamieson, A. M. *Macromolecules*, 1985, 18, 266.

- [21] Cametti, C.; Codastefano, P.; D'Amato, R.; Furlani, A.; Russo, M. V. *Synthetic Metals*, 2000,114, 173.
- [22] Cametti, C.; D'Amato, R.; Furlani, A.; Russo, M. V. *Chemical Physic Letters*, 2003,370, 602.
- [23] Lee, C. M.; Pearce, E. M.; Kwai, T. K. *Polymer*, 1996, 37, 4283.

## 5.8 CAPTION OF FIGURES

Figure 5.1 A synthesis route for H-chitosan

Figure 5.2 FT-IR spectra of (a) chitosan, and (b) H-chitosan,

Figure 5.3  $^1\text{H-NMR}$  spectrum of H-chitosan in  $\text{CDCl}_3$

Figure 5.4 The intrinsic viscosity of H-chitosan dissolved in (a) chloroform, (b) dichloromethane, and (c) tetrahydrofuran at  $30^\circ\text{C}$ .

Figure 5.5 Specific viscosity dependence of the product concentration-intrinsic viscosity for H-chitosan in three solvent investigated.

Figure 5.6 The apparent diffusion coefficient and diffusion coefficient of H-chitosan in three solvent investigated at different concentrations in (a-b) chloroform, (c-d) dichloromethane, and (e-f) tetrahydrofuran in dilute regime at  $30^\circ\text{C}$ .

Figure 5.7 The diffusion coefficient as the function of the viscosity of the solvent for H-chitosan in three solvent investigated.

Figure 5.8 Optical drop shape of H-chitosan solution dissolved in chloroform  
Variation of surface tension on concentration for H-chitosan in three solvent investigated.

Figure 5.9 Surface tension for H-chitosan in three solvent investigated

**Table 5.1** Properties of solvents

Properties	Chloroform	Dichloromethane	Tetrahydrofuran
Viscosity@30°C (cP)	0.539	0.440	0.460
Refractive index	1.443	1.424	1.407
Surface tension (mN/M)	27.50	28.60	26.40
Density (g/cm <sup>3</sup> )	1.483	1.327	0.889
Solubility parameter (Cal/cm <sup>3</sup> ) <sup>1/2</sup>	9.34	9.70	9.10



**Table 5.2** Molar volume and attraction constants [13]

Group	Molar volume constant, $V_i^*$ ( $\text{cm}^3 \text{mole}^{-1}$ )	Molar attraction constant, $F_i^*$ ( $(\text{cal.cm}^3)^{0.5} \text{mole}^{-1}$ )
-CH <sub>3</sub>	31.8	218
-CH <sub>2</sub> -	16.5	132
>CH-	1.9	23
-OCO-	19.6	298
-CO-	10.7	262
-O-	5.1	95
>N-	-0.5	-3

**Table 5.3** Intrinsic viscosity,  $[\eta]$  and Huggins coefficient,  $k_H$  for H-chitosan solutions dissolved in different organic solvents at 30°C

Solvent	$[\eta]$ (dl/g)	$k_H$
Chloroform	1.427±0.008	0.376±0.012
Dichloromethane	1.402±0.003	0.496±0.005
Tetrahydrofuran	1.385±0.003	0.508±0.003

**Table 5.4**  $D_o$ ,  $k_D$ ,  $\mu_2/\Gamma^2$  and  $R_H$  data obtained from dynamic light scattering measurement for H-chitosan solutions in different organic solvents at 30°C

Solvent	$D_o \times 10^7$ (m <sup>2</sup> /sec)	$R_H$ (nm)	$k_D$	$\mu_2/\Gamma^2$
Chloroform	8.21±0.0	50.12±0.2	15.24±0.6	0.61±0.03
Dichloromethane	13.11±0.4	38.51±1.2	16.73±1.3	0.40±0.07
Tetrahydrofuran	12.09±0.1	39.92±0.2	20.78±0.2	0.38±0.02

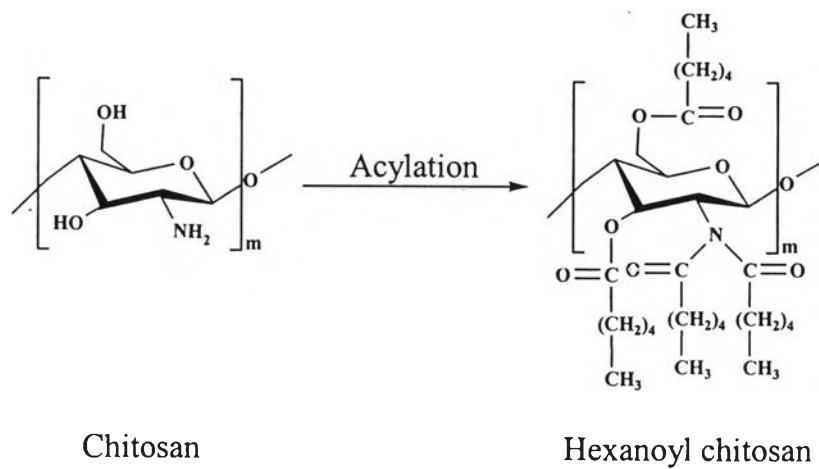


Figure 5.1

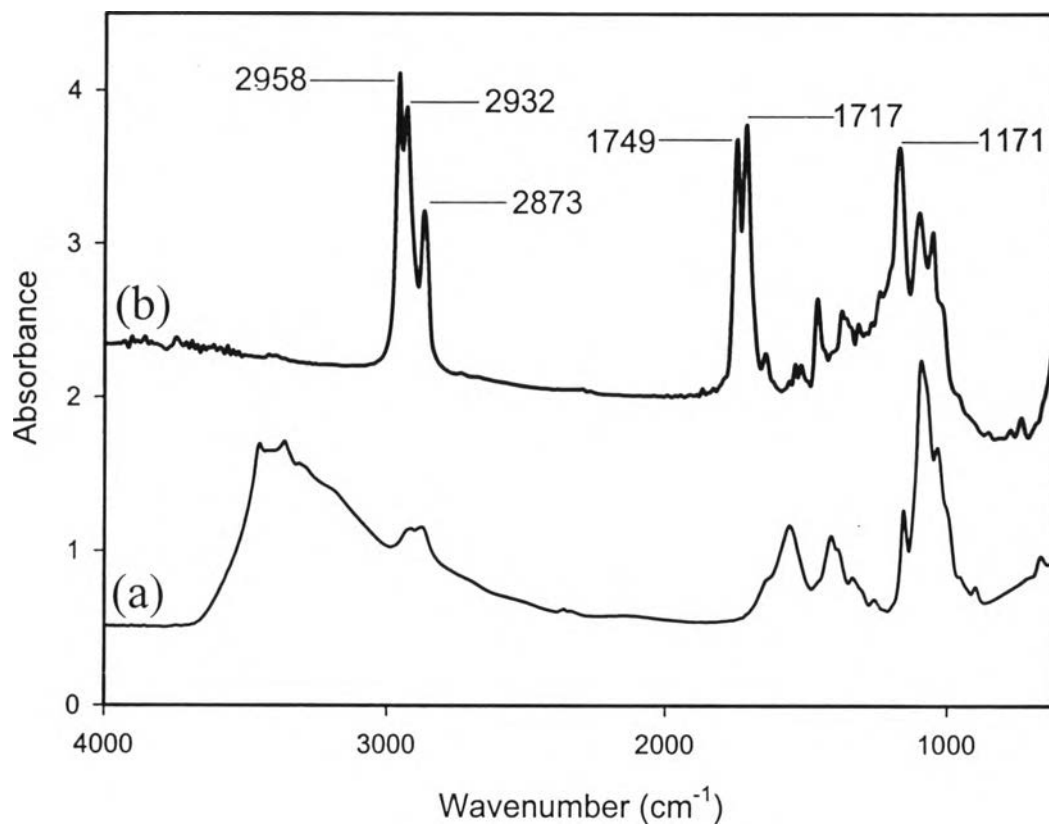


Figure 5.2

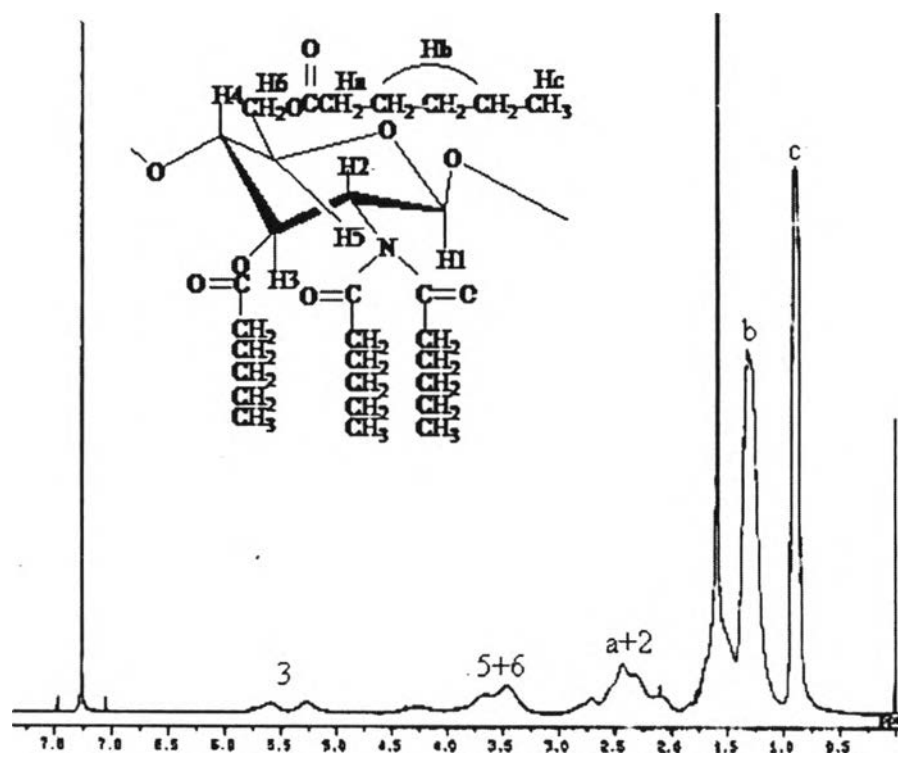
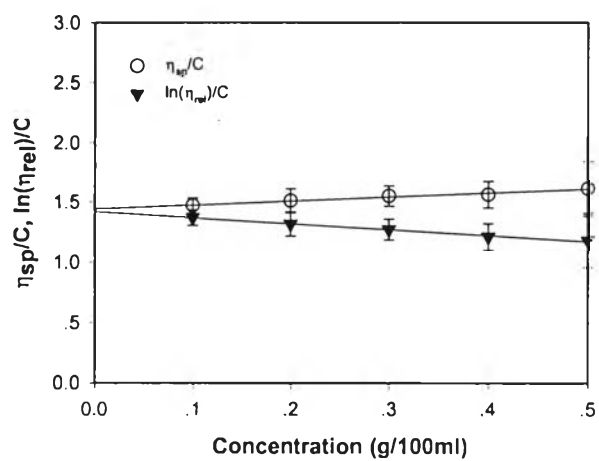
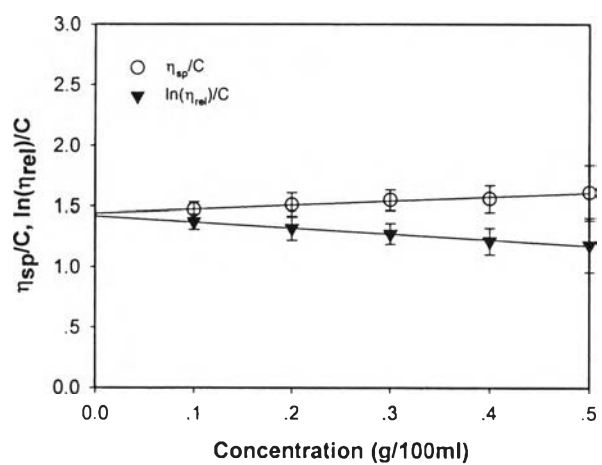


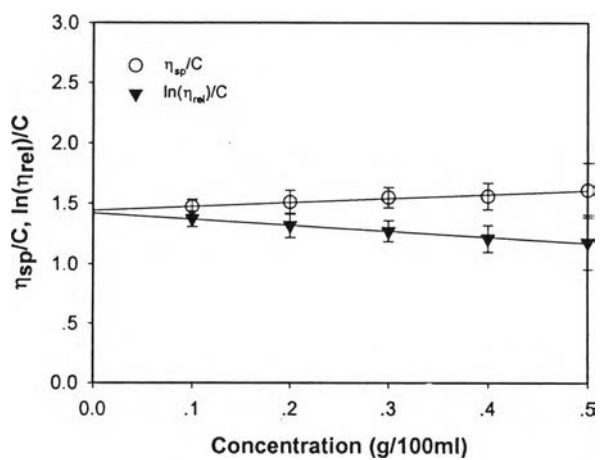
Figure 5.3



(a)



(b)



(c)

Figure 5.4

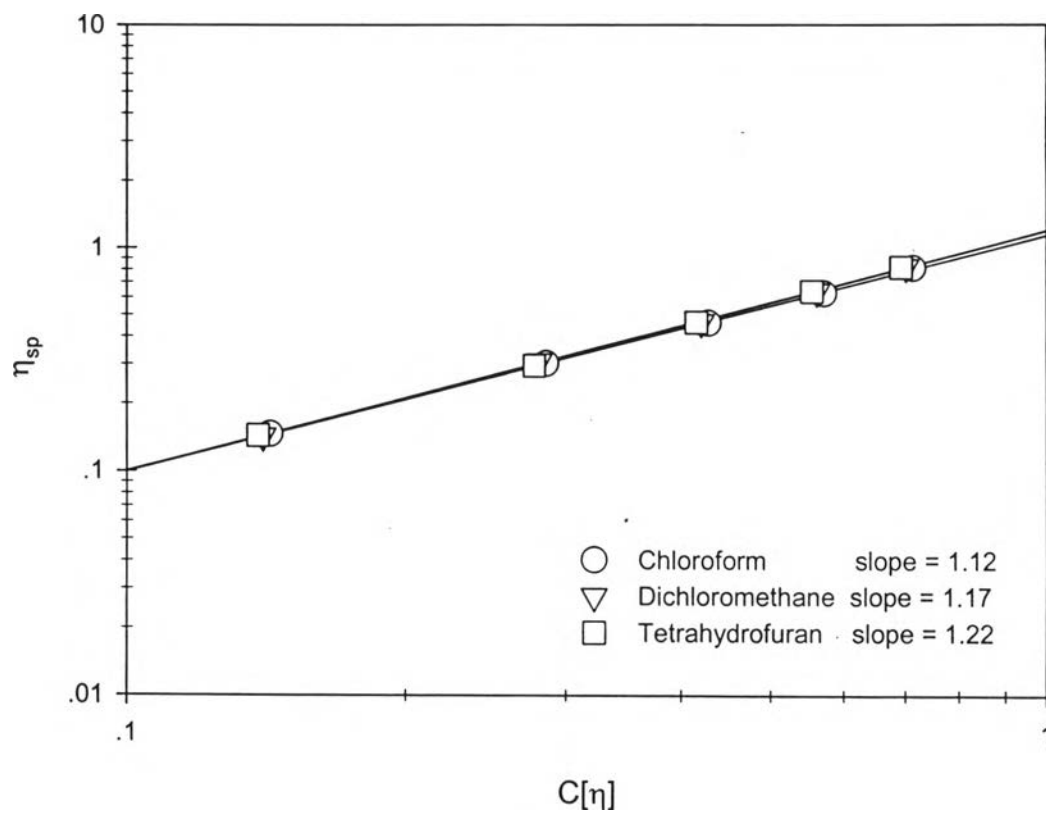
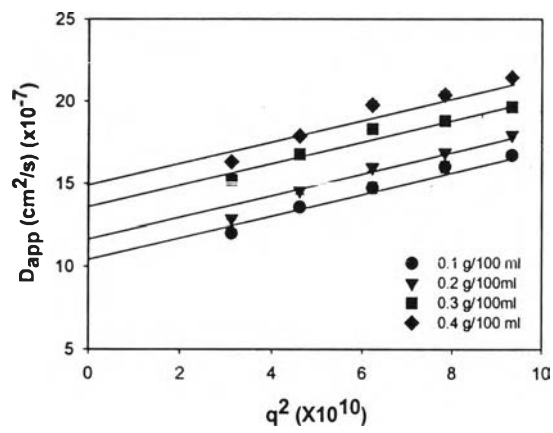
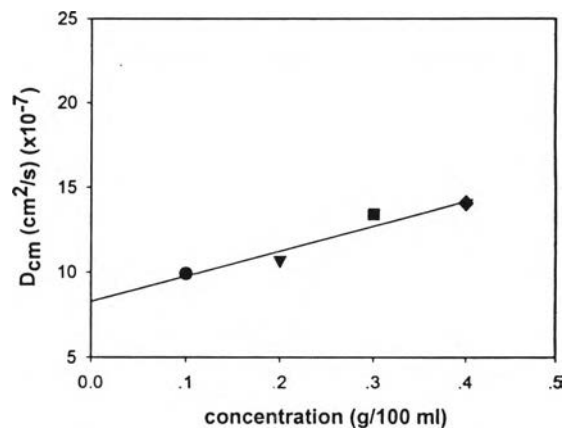


Figure 5.5

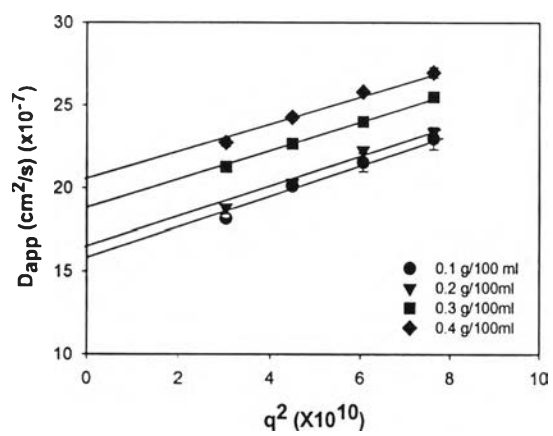




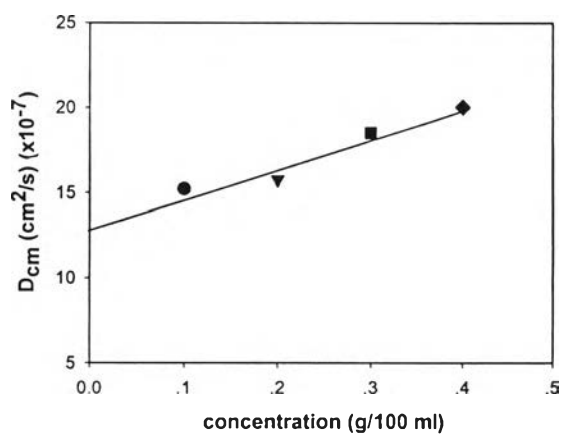
(a)



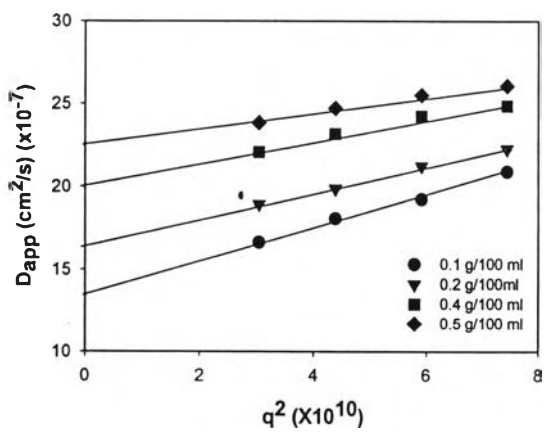
(b)



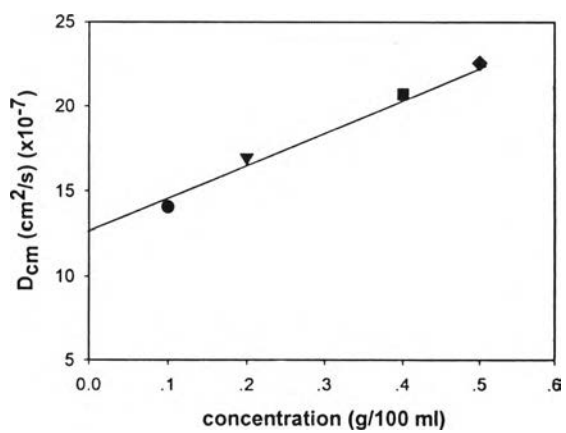
(c)



(d)



(e)



(f)

Figure 5.6

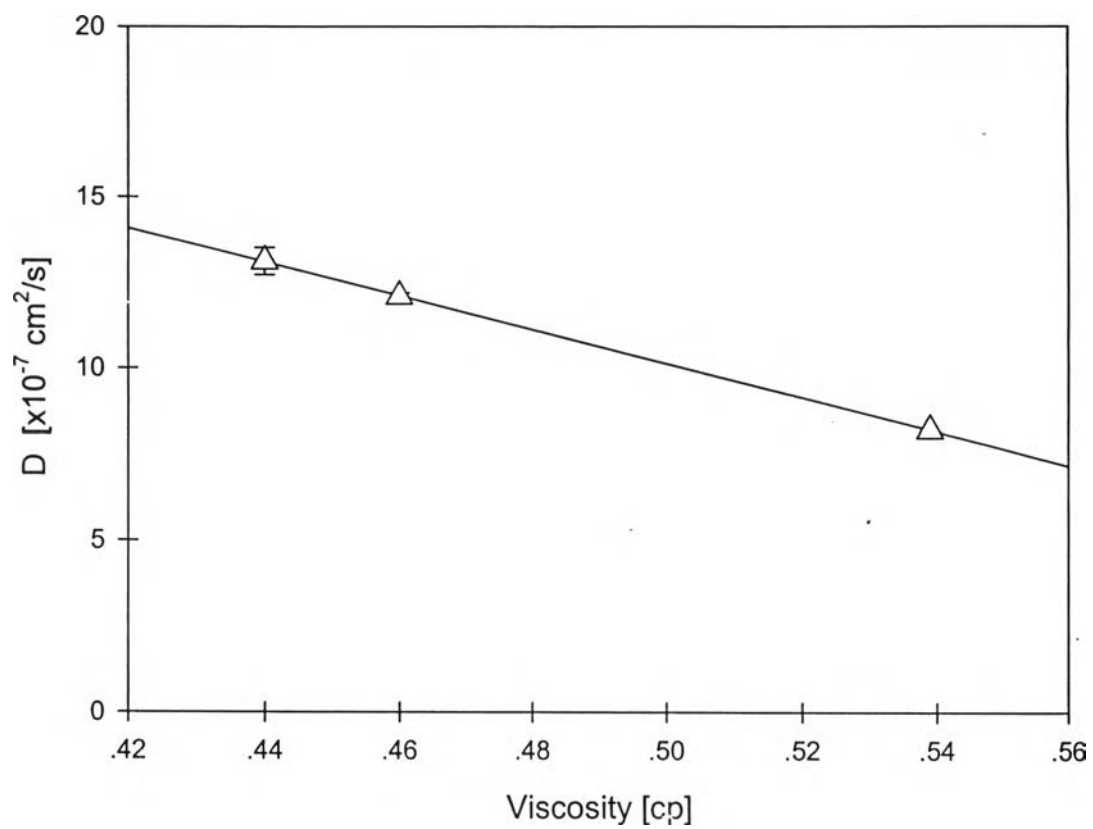
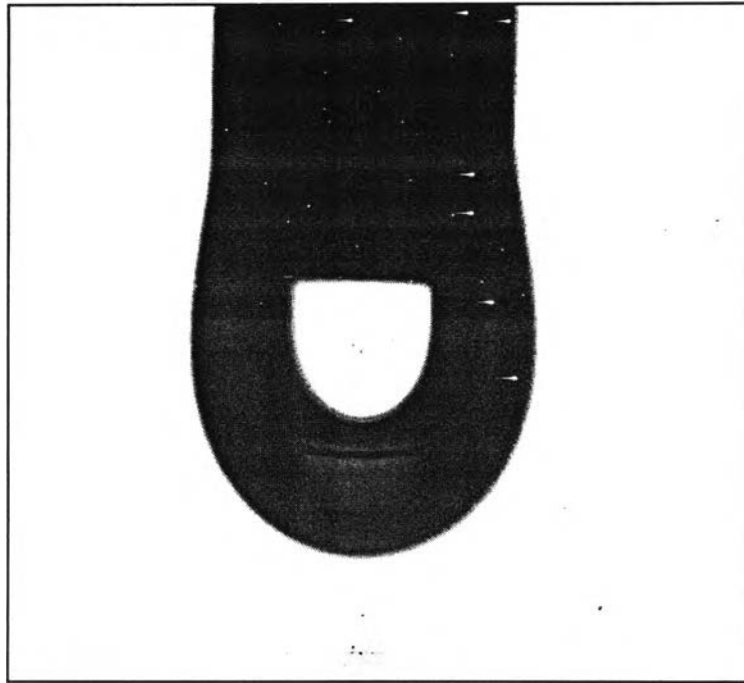


Figure 5.7



**Figure 5.8**

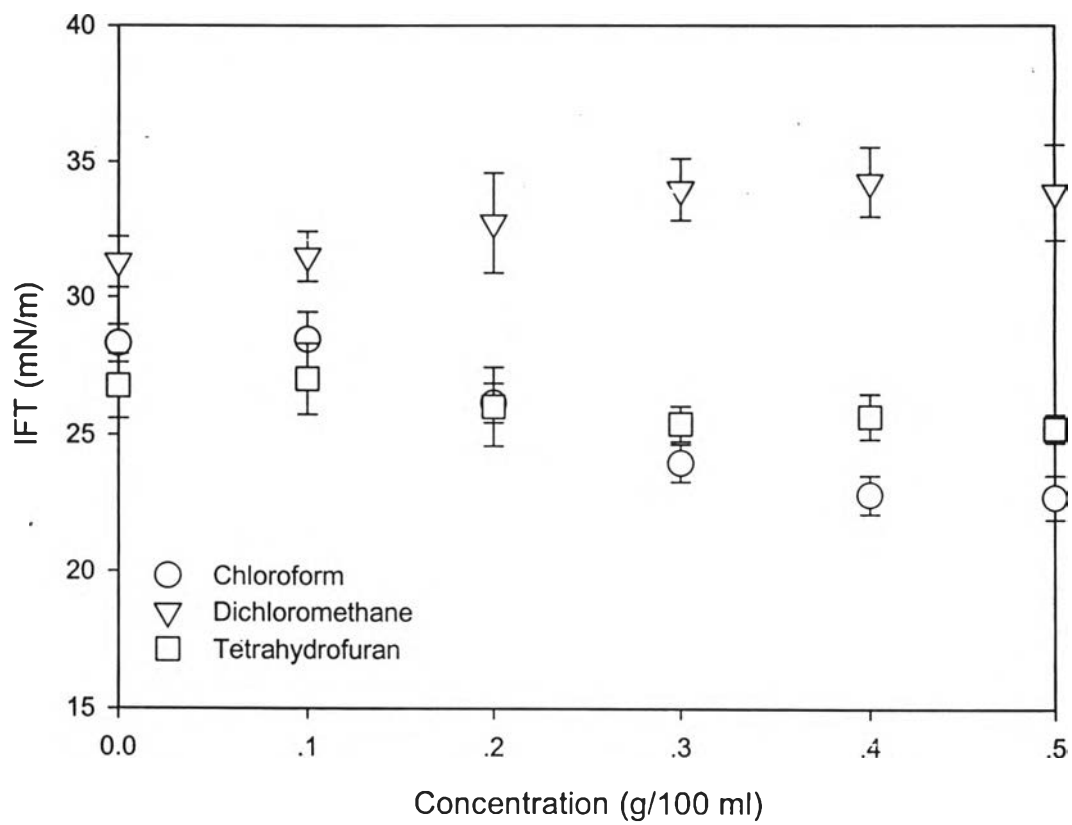


Figure 5.9